

Supporting Information

Programmable “triple attack” cancer therapy through *in situ* activation of disulfiram toxification combined with phototherapeutics

Qiu-Ling He,^{‡a} Ben-Xu Jia,^{‡ab} Zhi-Rong Luo,^{‡d} Yu-Kun Wang,^b Bo Zhang,^b Tao Liao,^a Xuan-Yi Guang,^b Yan-Fang Feng,^{*a} Zhen Zhang,^{*c} and Bo Zhou^{*ab}

^aSchool of Pharmacy, Guilin Medical University, Guilin, Guangxi, 541199, People’s Republic of China.

^bScientific Research Center, Guilin Medical University, Guilin, Guangxi, 541199, People’s Republic of China.

^cCollege of Intelligent Medicine and Biotechnology, Guilin Medical University, Guilin, Guangxi, 541199, People’s Republic of China.

^dCollege of Chemistry and Environmental Engineering, Baise University, Baise, Guangxi 533000, People’s Republic of China.

E-mail: zb090900021@163.com (B. Zhou), 1328468450@qq.com(Y.-F. Feng), zhenzhang@glmc.edu.cn (Z. Zhang).

‡ These authors contribute equally to the work.

Key words: disulfiram, residual tumor, programmable “triple attack” cancer therapy, “nontoxicity-to-toxicity” chemical chelation transformation, NIR-II phototherapeutics

Experimental section

Materials. Copper chloride dihydrate ($\text{CuCl}_2 \cdot 2\text{H}_2\text{O}$) was purchased from Sinopharm Chemical Reagent Co., Ltd. (China). Disulfiram (DSF), sodium thiosulfate pentahydrate ($\text{Na}_2\text{S}_2\text{O}_3 \cdot 5\text{H}_2\text{O}$), poly-(vinylpyrrolidone) (PVP, K30), tannic acid (TA) and rhodamine 6G (R6G) were obtained from Shanghai Aladdin Bio Chemical Technology Co., Ltd. (China). Dulbecco's modified Eagle's medium (DMEM), RPMI-1640 and fetal bovine serum (FBS) were ordered from Thermo Fisher Scientific (USA). 4'-6-diamidino-2-phenylindole (DAPI), antifade Mounting Medium and calcein-AM/PI double staining Kit were provided by Beyotime Biotechnology Co., Ltd. (China). Phosphate buffer solution (PBS), trypsin-EDTA, dimethyl sulfoxide (DMSO), penicillin-Streptomycin Liquid (100 \times), methyl thiazolyl diphenyl-tetrazolium bromide (MTT) were bought from Beijing Solarbio Science & technology Co., Ltd. (China). Methanol and formaldehyde were supplied by Kelong Chemical Reagent Co., Ltd. (China). All chemical reagents were purchased from commercial sources and used without further purification. Deionized water with a resistivity higher than 18 M Ω cm was used in all relevant experiments.

Characterization. The morphology of nanomaterials were obtained on transmission electron microscopy (TEM, HT770, Hitachi, Japan). Hydrodynamic diameter and zeta potentials were measured by dynamic light scattering (DLS, Zetasizer Nano ZS-90, Malvern, UK). UV-vis adsorption spectra were investigated by UV-vis spectrophotometer (UV-2401PC, Shimadzu, Japan). The functional groups were identified by Fourier-transform infrared spectroscopy (FTIR, Thermo Fisher Scientific, USA). The composition of elements and valence state of Cu was performed on X-ray photoelectron spectroscopy (XPS, Thermo Fisher Scientific, USA).

The crystal structure were characterized by X-ray diffractometer (XRD, Bremen, Germany). The amount of Cu was determined by inductively coupled plasma atomic emission spectroscopy (ICP-OES, Optima7000 and Avio from PerkinElmer, USA).

Synthesis of CuS@TA. CuS@TA nanohexahedrons were prepared *via* one step hydrothermal method. Briefly, $\text{CuCl}_2 \cdot 2\text{H}_2\text{O}$ (0.1022 g) and PVP K30 (3.0 g) were dissolved in 20 mL deionized water and stirred until clear. Then, 10 mL TA (5 mg mL^{-1}) and $\text{Na}_2\text{S}_2\text{O}_3 \cdot 5\text{H}_2\text{O}$ (72.5 mg mL^{-1}) mixed solution was added into the above mixture in turn. After that, the mixture was transferred into Teflon-lined autoclave, heated up to $140 \text{ }^\circ\text{C}$ and continue for another 6 h. After cooling down to the room temperature, the reactant was filtered and centrifuged at 13000 rpm for 10 min, washed with ultrapure water 3 times. Then, the obtained CuS@TA were dried at $50 \text{ }^\circ\text{C}$.

DSF Loading. Briefly, 1 mL of CuS@TA (1 mg mL^{-1}) methanol solution was mixed with 1 mL of DSF (29.65, 59.30, 88.95, 118.60, 148.25, 177.90, 207.55, 237.20, 266.85, 296.50 $\mu\text{g mL}^{-1}$) methanol solution at room temperature. After 2 h stirring, the mixture was centrifuged (13000 rpm, 10 min) to obtain DSF-CuS@TA. Then, the supernatant was collected, and excessive Cu^{2+} was added to the supernatant to chelate with DSF that did not participate in the reaction to form $\text{Cu}(\text{DTC})_2$. After a certain time, the absorbance at 425 nm was determined, the amount of DSF that did not participate in the reaction, as well as DSF loading efficiency (LE) and encapsulation efficiency (EE) were calculated according to the absorbance at 425 nm and the standard curve The LE and EE of DSF loading on CuS@TA were calculated by using the following equations:¹

$$LE(\%) = \frac{\text{total mass of DSF} - \text{DSF in supernatant}}{\text{total mass of CuS@TA}} \times 100\%$$

$$EE(\%) = \frac{\text{total mass of DSF} - \text{DSF in supernatant}}{\text{total mass of DSF}} \times 100\%$$

R6G Loading. In order to evaluate the cell uptake efficiency of CuS@TA, fluorescent reagent R6G was loaded into CuS@TA. The synthesis method of R6G-CuS@TA is similar to DSF-CuS@TA, except for replacing DSF with R6G.

Physiological stability evaluation. DSF-CuS@TA was incubated with different media (water, saline, PBS and 1640 medium). Then 1 mL of sample solution were collected from each media at given times (0, 1, 2, 4, 6, 8, 10, 12, 24 h) for particle size measurement.

Photothermal and photoacoustic imaging performance of DSF-CuS@TA. Firstly, CuS@TA, DSF-CuS@TA (20 $\mu\text{g mL}^{-1}$) solution and pure water were exposed to 1064 nm laser irradiation (1.0 W cm^{-2}) for 10 min. The temperature changes were detected by temperature loggers and photothermal images were recorded by thermal camera. Subsequently, the temperature curves with variable power intensities and concentrations were also measured (1064 nm, 10 min). In the experiment of photothermal stability, 1 mL of 20 $\mu\text{g mL}^{-1}$ DSF-CuS@TA solution was exposed to 1064 nm laser (1.0 W cm^{-2}) irradiation for 10 min, then, the laser was turned off to cool down for 15 min, the rising and falling temperature curves were obtained by repeating five times. The photothermal conversion efficiency of 20 $\mu\text{g mL}^{-1}$ DSF-CuS@TA with 1064 nm laser irradiation was calculated as the following equation:²

$$\eta = \frac{hs(T_{max} - T_{surr}) - Q_{dis}}{I(1 - 10^{-A_{1064}})}$$

The photoacoustic imaging performance of DSF-CuS@TA was evaluated by the MSOT imaging system (MSOT in Vision 128, iTheramedical). DSF-CuS@TA nanoparticles with

different concentrations (50, 100, 200, 400 $\mu\text{g mL}^{-1}$) were dispersed in water, and pure water was used as the control group. Photoacoustic signals were collected by the MSOT imaging system.

Multiple stimulus response degradation of CuS@TA. In order to analyze the biodegradation effect of CuS@TA at different pH and temperatures, CuS@TA was dissolved in PBS solution (100 $\mu\text{g mL}^{-1}$) with the pH 6.5 and 7.4, and incubated under 4 °C, 37 °C, and 55 °C, respectively. Subsequently, 1 mL sample solution was taken out at given times (0, 4, 8, 12, and 24 h), and the absorbance at 1064 nm was measured by UV-vis spectrophotometer. Furthermore, the particle size and morphology of CuS@TA at different time intervals (0, 4, and 7 days) were measured by DLS and TEM, respectively.

Cu²⁺ release. To further evaluate the multiple stimuli-response degradation behavior of CuS@TA, CuS@TA was dissolved in PBS solution with pH of 6.5 and 7.4. The release procedure was conducted in different temperatures (4 °C, 37 °C, and 55 °C). Then, 1 mL of sample solution was collected at the given time points and centrifuged, the contents of Cu²⁺ in the supernatant was measured by ICP-OES.

Formation of Cu(DTC)₂. DSF-CuS@TA was immersed in PBS solution (100 $\mu\text{g mL}^{-1}$) with a pH of 6.5 and 7.4 under variable temperatures (4 °C, 37 °C, and 55 °C). Then 1 mL of sample solution was taken out at the given times (0, 4, 8, 12, and 24 h) and the absorbance at 425 nm was measured by UV-vis spectrophotometer.

Cell lines and Cells culture. Mouse breast cancer (4T1) cells, human liver cells (L02), human kidney cells (293T), mouse melanoma cells (B16) and human breast cancer cells (MDA-MB-

231) were acquired from the Chinese Academy of Sciences Cell Bank (Shanghai, China). MDA-MB-231, 293T and L02 cells were incubated in DMEM medium supplemented 10% fetal bovine serum (FBS) and 1% penicillin/streptomycin at 37 °C under 5% CO₂ atmosphere. 4T1 and B16 cells were cultured in RPMI-1640 supplemented with similar supplements and cultured as above methods.

Cellular uptake. To investigate the cellular uptake of materials, R6G-CuS@TA was used as an imaging probe for the detections. Firstly, 4T1 cells were incubated at a density of 2.5×10^5 cells/well for 24 h in six-well plates containing crawlers. Then the cells were incubated with fresh medium containing R6G-CuS@TA (0.5 mL, $20 \mu\text{g mL}^{-1}$). After incubating for 0, 4, 8 and 12 h, the cells were washed with PBS (3 \times) and stained with DAPI (100 μL) for 15 minutes. After that, the cells were washed with PBS (3 \times) and blocked with anti-fluorescence quencher. Finally, the cells were observed on confocal laser-scanning microscopy (CLSM) to observe the uptake of R6G-CuS@TA. In addition, the intracellular Cu²⁺ content was determined by ICP-OES after the incubation of the cells with CuS@TA for 12 h.

***In vitro* cytotoxicity evaluation.** The cell viability of 4T1, MDA-MB-231, B16, 293T and L02 were evaluated by MTT assay. The MTT experiment of 4T1 cells was taken as an example. Firstly, 4T1 cells were seeded in 96-well plates (1×10^4 cells per well) and cultured in 37 °C, 5% CO₂ for 24 h. Subsequently, 100 μL 1640 basic culture medium containing different concentrations of DSF, CuS@TA and DSF-CuS@TA were added into each well under pH values of 7.4 and 6.5. The Cu(DTC)₂ group shared with the same concentration of DSF. After incubated with the cells for 12 or 24 h, 10 μL of MTT (5 mg mL^{-1}) was added and incubated for another 4 h. The supernatant was pipetted out slowly and 100 μL of DMSO was added into

each well to dissolve the purple crystals. Finally, the absorbance of the 96-well plate at 490 nm was measured by microplate reader.

Meanwhile, the cell-level of *in situ* chemo-photothermal therapy effects were also evaluated. Typically, The 4T1 cells were subjected to eight treatment groups, including control, Laser only, CuS@TA only (20 $\mu\text{g mL}^{-1}$), DSF only (20 $\mu\text{g mL}^{-1}$), CuS@TA+Laser, DSF-CuS@TA (20 $\mu\text{g mL}^{-1}$), Cu(DTC)₂ (20 $\mu\text{g mL}^{-1}$) and DSF-CuS@TA+Laser. After incubated 24 h, the cells were exposed to 1064 nm laser at the power intensity of 1.0 W cm⁻² for 10 min and incubated for another 0, 6, 12 h. After that, the supernatant was pipetted out slowly and 100 μL of DMSO was added into each well to dissolve the purple crystals. Finally, the absorbance of the 96-well plate at 490 nm was measured by microplate reader. The cell viability was calculated according to the follow equation:

$$\text{Cell viability}(\%) = \frac{A_{\text{sample}} - A_{\text{blank}}}{A_{\text{control}} - A_{\text{blank}}} \times 100\%$$

Live-dead cell staining assay. The 4T1 cells were cultured in CLSM special glass dish ($\varphi=20$ mm, 2×10^5 cells per dish) for 24 h. Then, the cells were given various treatments under pH values of 6.5 and 7.4, including control, Laser only, CuS@TA only, DSF only, CuS@TA+Laser, DSF-CuS@TA, Cu(DTC)₂ and DSF-CuS@TA+Laser for another 24 h. Then, the cells with the laser groups were exposed to 1064 nm laser (1.0 W cm⁻²) irradiation for 10 min and incubated another 0, 6, 12 h. Next, the cells washed with PBS (3 \times) and incubated with Calcein-AM/PI (200 μL) for 15 min. Finally, the cells were washed with PBS (3 \times) and visualized by CLSM. The surviving cells showed green fluorescence ($\lambda_{\text{ex}}=490$ nm, $\lambda_{\text{em}}=515$ nm), and the dead cells emitted red fluorescence ($\lambda_{\text{ex}}=535$ nm, $\lambda_{\text{em}}=617$ nm).³

Cell apoptosis analysis. The 4T1 cells were cultured in six-well plate (2×10^5 cells per plate)

for 24 h and exposed to various treatments, including control, Laser, CuS@TA, DSF, CuS@TA+Laser, DSF-CuS@TA, Cu(DTC)₂ and DSF-CuS@TA+Laser. After the cells were initially treated with PBS, CuS@TA or DSF-CuS@TA for 24 h, the cells was irradiated with 1064 nm laser (1.0 W cm⁻²) for 10 min and incubated with another 0, 6, 12 h. Then, the cells were trypsinized, centrifuged, washed with PBS and incubated with Annexin V-FITC/PI for 20 min. Finally, the cells were analyzed by flow cytometry.

Animal experiment. An experimental animal model using SPF grade female BALB/c mice was provided by Hunan Slack Jingda Laboratory Animal Co. All animal experiments were performed in accordance with the guidelines of Institutional Animal Care and Use Committee and approved by the Laboratory Animal Care and Animal Ethics Committee of Guilin Medical University (No. GLMC-IACUC-2022027).

Establishment of tumor model *in vivo*. 4T1 cells (1×10⁶ cells, 100 μL) were injected into the right abdomen of nude mice to establish the animal tumor model. The following experiments were performed when the tumor volume reached approximately 100 mm³.

***In vivo* fluorescence imaging.** The 4T1 tumor-bearing nude mice were administrated with an intravenous injection of R6G-CuS@TA, Subsequently, the fluorescence was monitored at various time points after injection by using *in vivo* imaging system (IVIS). Finally, after injection 12 h, the mice were sacrificed and the fluorescence of main organs (heart, liver, spleen, lung and kidney) and tumors were measured.

Photoacoustic (PA) imaging *in vivo*. The PA imaging ability of DSF-CuS@TA *in vivo* was evaluated by the MSOT imaging system. Firstly, the tumor-bearing mice received intravenous

administration of DSF-CuS@TA (20 mg kg⁻¹), then, the PA signals in the tumor regions were recorded at determined time points postinjection (0, 2, 4, 6, 8, and 12h).

In vivo photothermal performance of DSF-CuS@TA. Saline (100 μL), CuS@TA (100 μL, 20 mg kg⁻¹), and DSF-CuS@TA (100 μL, 20 mg kg⁻¹) were injected into 4T1 tumor-bearing mice, respectively. After 12 h postinjection, the tumors of the mice were irradiated by a 1064 nm laser (1.0 W cm⁻², 10 min). The tumor temperature changes were recorded by temperature loggers, and the photothermal images were recorded by a thermal camera.

In vivo synergistic antitumor assay. To assess the treatment effect, 4T1 tumor-bearing nude mice (n = 24) with tumor volumes of about 100 mm³ were randomly divided into 8 groups (n = 3), including control, Laser, CuS@TA (20 mg kg⁻¹), DSF (20 mg kg⁻¹), CuS@TA+Laser, DSF-CuS@TA (20 mg kg⁻¹), Cu(DTC)₂ (20 mg kg⁻¹), and DSF-CuS@TA+Laser groups. The drugs injection were given once every three days and the laser irradiation (1.0 W cm⁻², 10 min) was performed after 12 h post-injection. The tumor size and body weight of the mice were measured on alternate days, and the tumor volume was calculated according to the formula:

$$V = \frac{L \times W^2}{2}$$

The changes in tumor size were evaluated by comparing the relative tumor volume (V/V₀, where V₀ is the initiate tumor volume before treatment). After treatment for 14 days, the mice were sacrificed, the main organs (heart, liver, spleen, lung and kidney) and tumor were harvested and used for H&E staining.

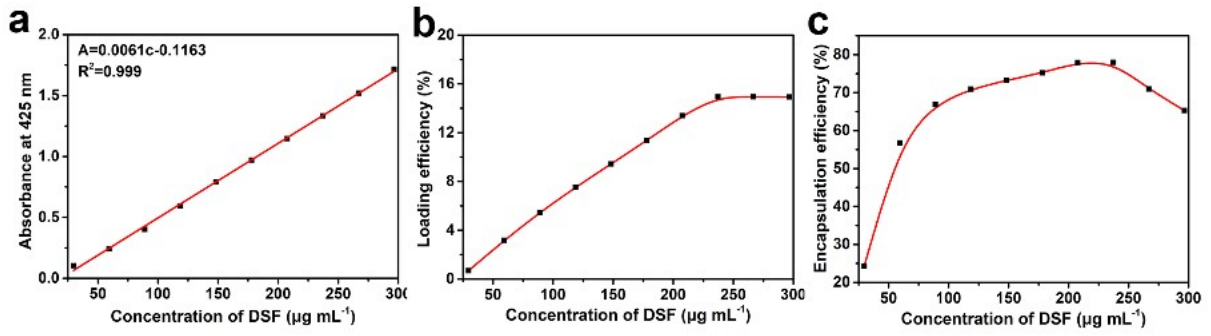


Fig. S1 (a) Standard curve of Cu^{2+} -DSF. (b) Loading efficiency and (c) encapsulation efficiency of DSF.

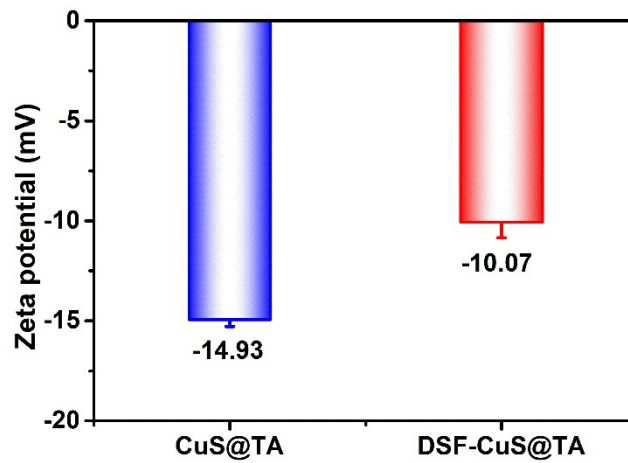


Fig. S2 Zeta potential of CuS@TA and DSF-CuS@TA .

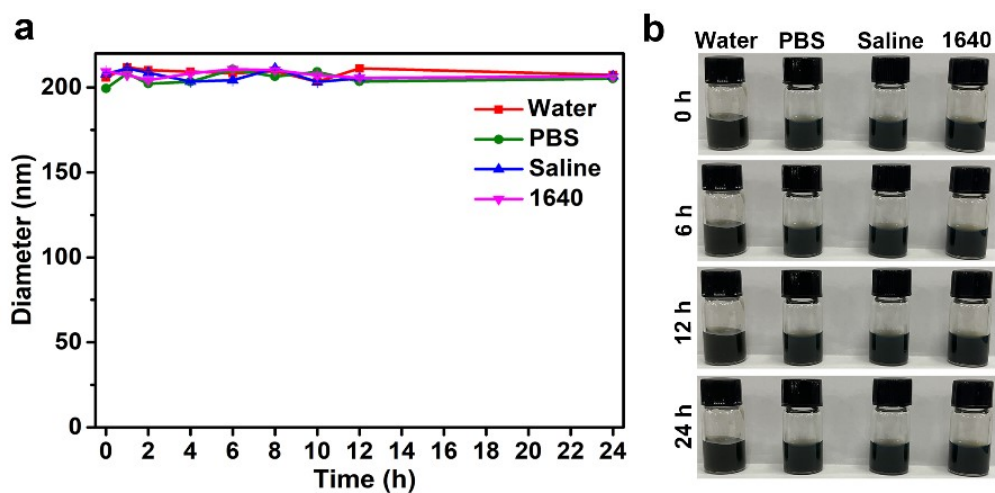


Fig. S3 (a) Hydrodynamic size and (b) photograph of DSF-CuS@TA dispersed in different media within 24 h.

Table S1 Content of C 1s and S 2p element in CuS@TA and DSF-CuS@TA.

	C 1s	S 2p
CuS@TA	40.48%	22.35%
DSF-CuS@TA	45.57%	25.94%

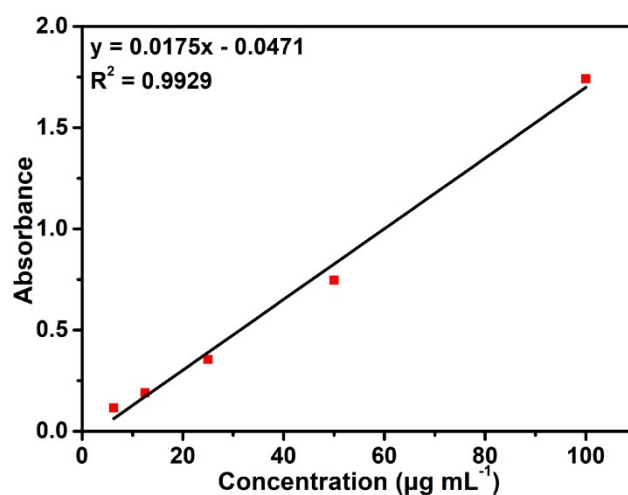


Fig. S4 The fitting curve of extinction coefficient of CuS@TA at 1064 nm.

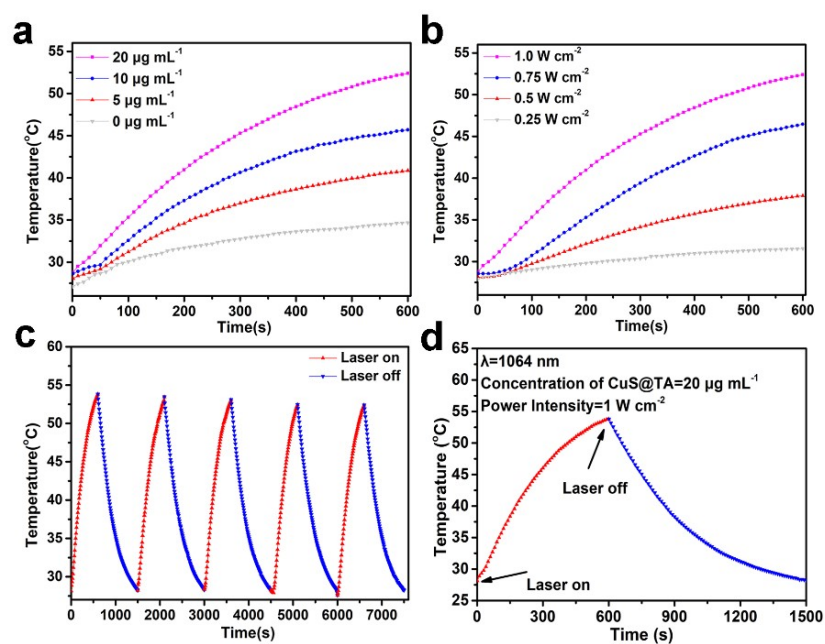


Fig. S5 (a) Heating curves of varying concentrations of CuS@TA aqueous dispersion upon 1064 nm laser exposure (1.0 W cm^{-2}). (b) Heating curves of a CuS@TA aqueous dispersion upon 1064 nm laser exposure at varying power densities. (c) Heating curve of a CuS@TA aqueous dispersion under five cycles of heating and cooling processes. (d) Photothermal conversion capability of a CuS@TA aqueous dispersion upon 1064 nm laser exposure (1.0 W cm^{-2}).

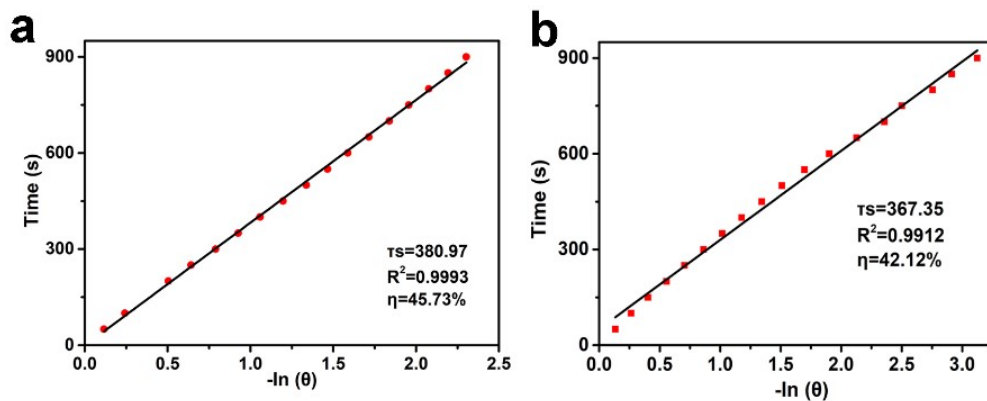


Fig. S6 Calculating curve of photothermal conversion efficiency of $20 \mu\text{g mL}^{-1}$ (a) DSF-CuS@TA and (b) CuS@TA irradiated at 1064 nm (1.0 W cm^{-2} , 10 min).

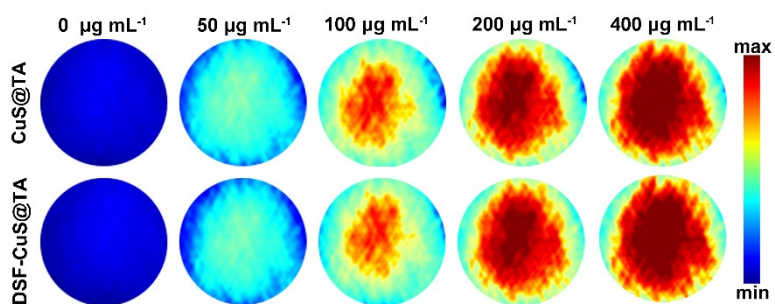


Fig. S7 Photoacoustic signal diagram of CuS@TA and DSF-CuS@TA at different concentrations.

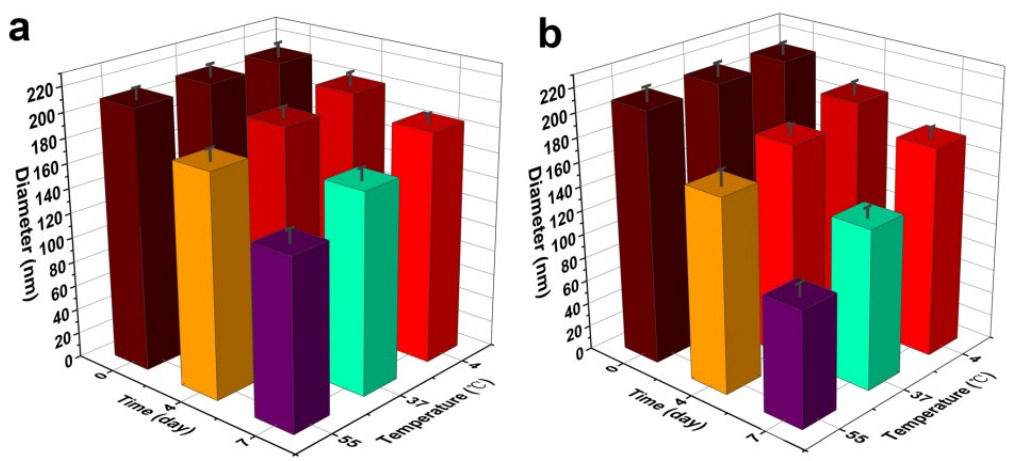


Fig. S8 Thermal- and pH- triggered degradation characteristics of DSF-CuS@TA, the hydrodynamic size of DSF-CuS@TA at (a) pH 7.4 and (b) pH 6.5.

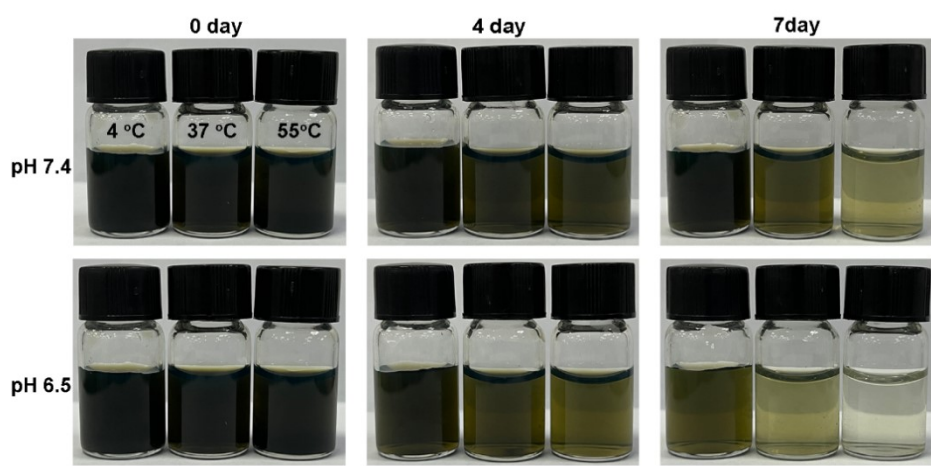


Fig. S9 The photograph of CuS@TA treated at different time points at pH 7.4/6.5, 55 °C.

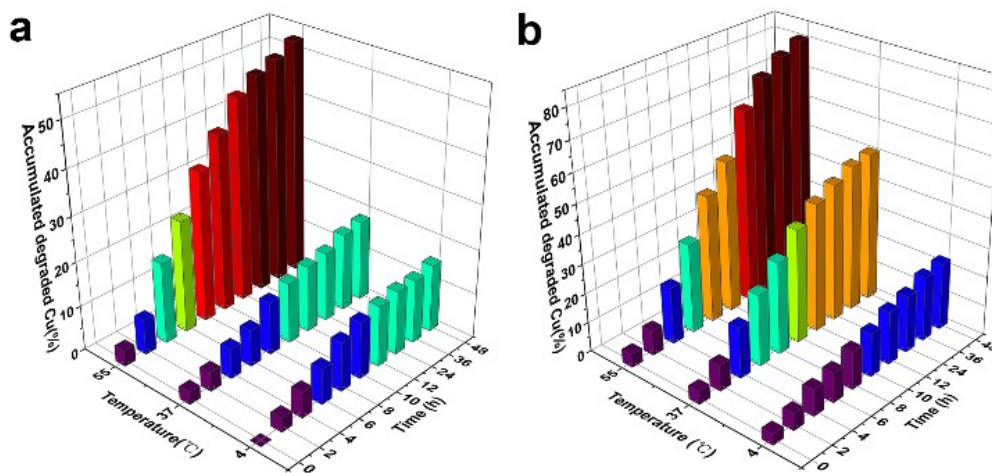


Fig. S10 Accumulative releasing profiles of biodegraded Cu^{2+} from CuS@TA in PBS solution at (a) pH 7.4 and (b) pH 6.5.

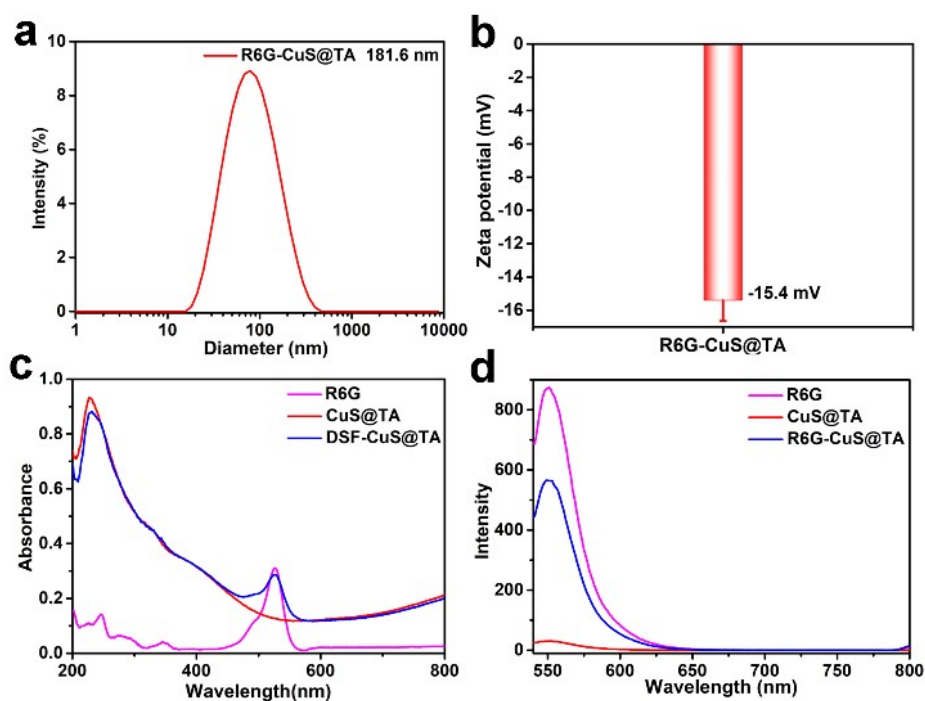


Fig. S11 (a) Hydrodynamic diameter, (b) zeta potential, (c) Uv-vis and (d) fluorescence spectra of R6G-CuS@TA .

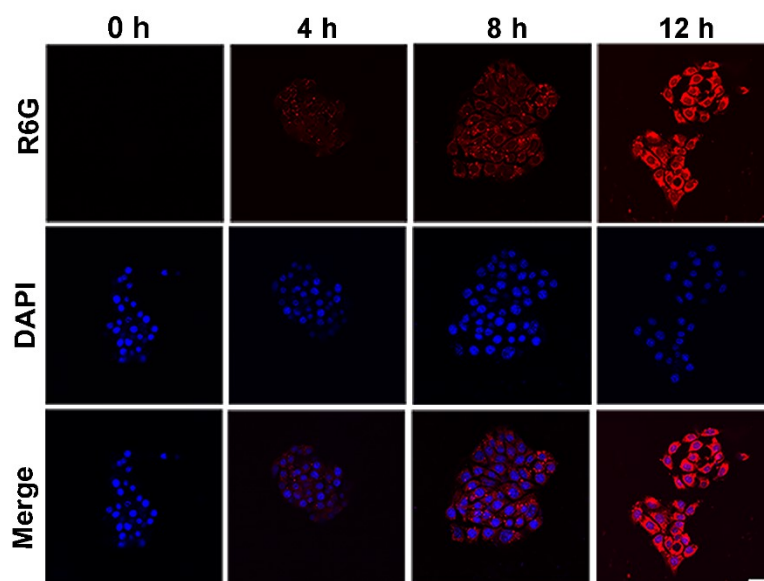


Fig. S12 CLSM images of 4T1 cells after co-culture with R6G-CuS@TA for different times.

Scale bar, 50 μm .

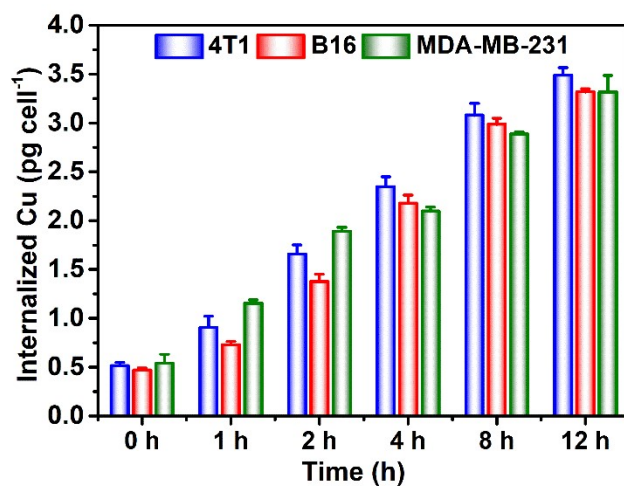


Fig. S13 Cellular internalization concentrations of Cu^{2+} in 4T1, B16, and MDA-MB-231 cancer cells after varied incubation durations by ICP-OES analysis.

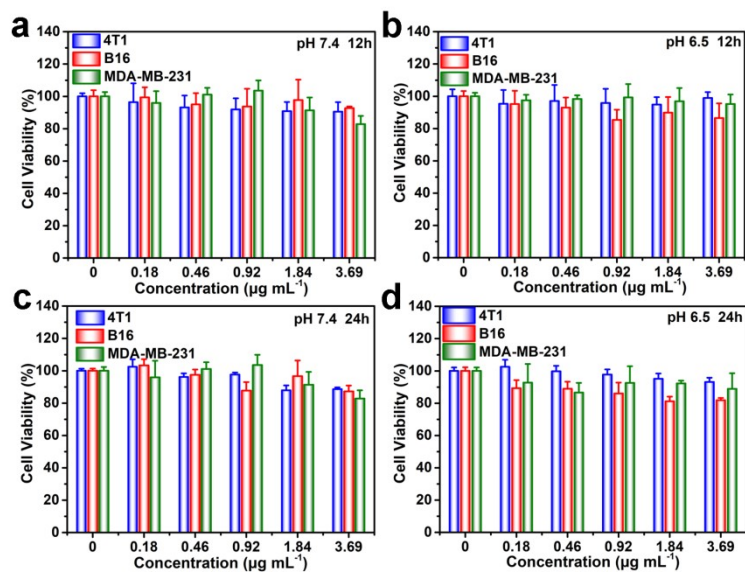


Fig. S14 Cell viability of 4T1, B16, and MDA-MB-231 cells treated with different doses of DSF (the concentration of DSF is equivalent to the load of DSF-CuS@TA) for different time under different pH conditions: (a) pH 7.4, 12 h, (b) pH 6.5, 12 h, (c) pH 7.4, 24 h and (d) pH 6.5, 24 h.

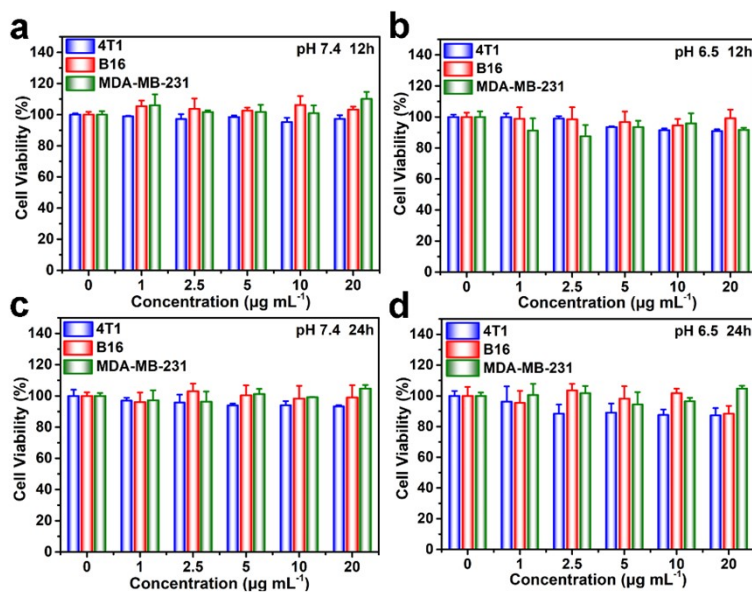


Fig. S15 Cell viability of 4T1, B16, and MDA-MB-231 cells treated with different doses of CuS@TA for different time under different pH conditions: (a) pH 7.4, 12 h, (b) pH 6.5, 12 h, (c) pH 7.4, 24 h and (d) pH 6.5, 24 h.

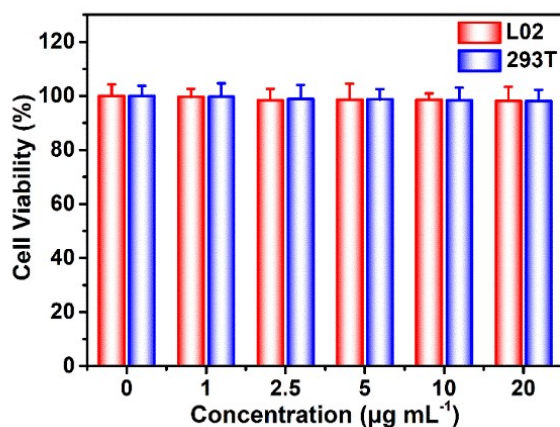


Fig. S16. The effects of different concentrations of DSF-CuS@TA incubation under pH 7.4 for 24 h on the viability of L02 and 293T.

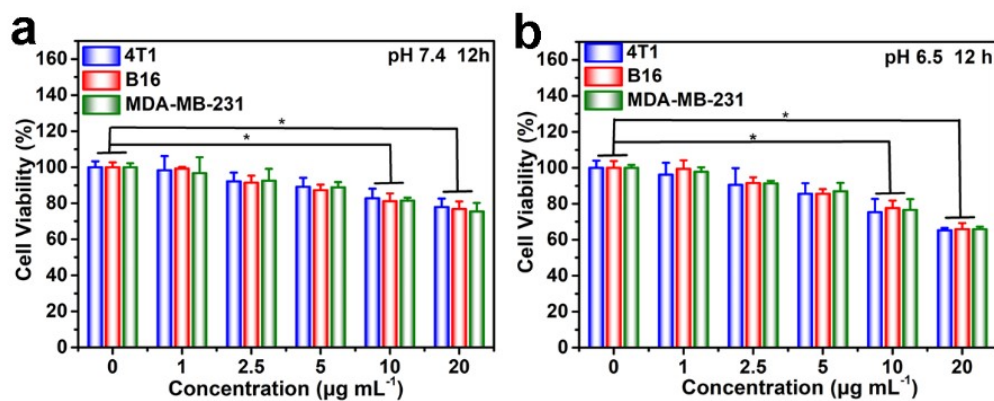


Fig. S17 Cell viability of 4T1, B16, and MDA-MB-231 cells treated with different doses of DSF-CuS@TA for 12 h under (a) pH 7.4 and (b) pH 6.5. Statistical significances were calculated *via* Student t-test. * $p < 0.05$.

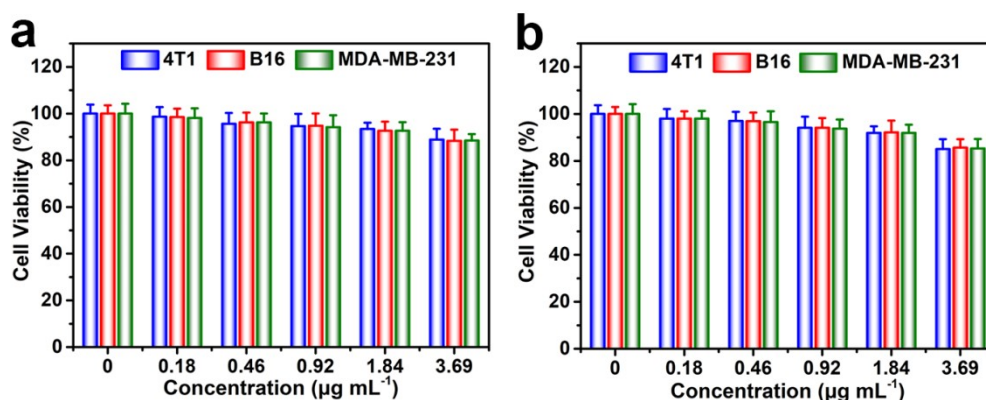


Fig. S18 Cell viability of 4T1, B16, and MDA-MB-231 cells treated with different doses of DSF (the concentration of DSF is equivalent to the load of DSF-CuS@TA) for 24 h under different pH conditions, followed by 1064 nm laser irradiation for 10 min: (a) pH 7.4 and (b) pH 6.5.

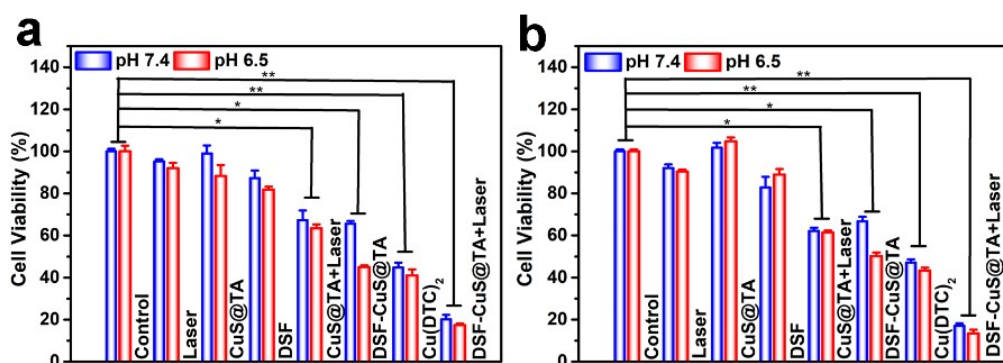


Fig. 19 Relative cell survival of (a) B16 cells and (b) MDA-MB-231 cells after different treatments, including control, Laser, DSF, CuS@TA, CuS@TA+Laser, DSF-CuS@TA, Cu(DTC)₂ and DSF-CuS@TA+Laser group. Statistical significances were calculated *via* Student t-test. * $p < 0.05$, and ** $p < 0.01$.

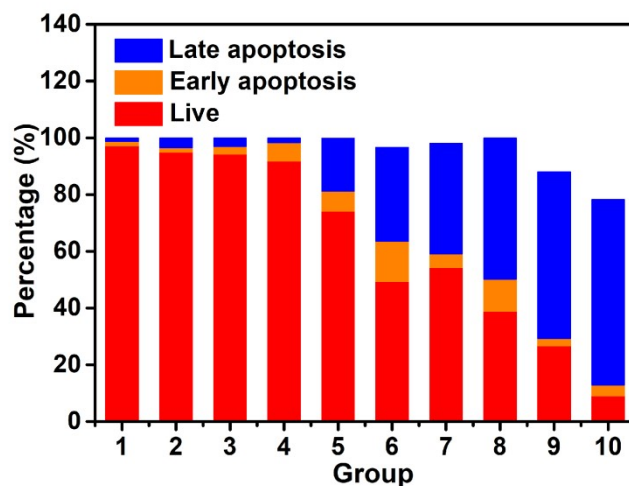


Fig. S20 The percentage of live, early apoptosis and late apoptosis cells in different treatment groups. (1: Control (treated with PBS), 2: Laser, 3: CuS@TA, 4: DSF, 5: CuS@TA+Laser, 6: DSF-CuS@TA, 7: Cu(DTC)₂, 8: DSF-CuS@TA+Laser-0 h, 9: DSF-CuS@TA+Laser-6 h, 10: DSF-CuS@TA+Laser-12 h groups).

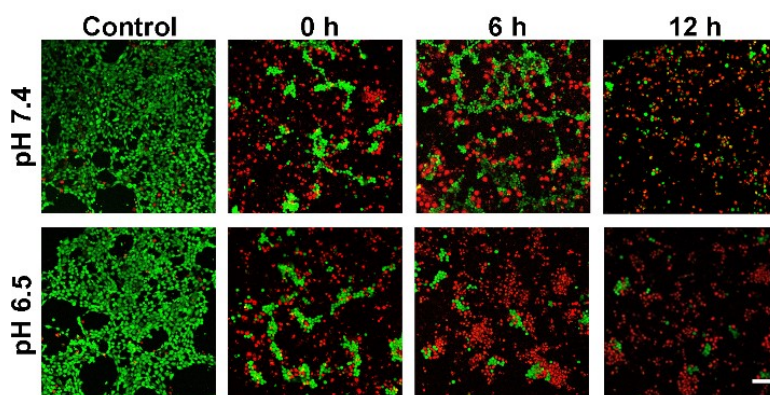


Fig. S21 Calcein-AM and PI-labeled CLSM images of 4TI cells treated with DSF-CuS@TA+Laser after incubation for 0, 6 and 12 h at pH 7.4 and pH 6.5, Scale bar, 100 μ m.

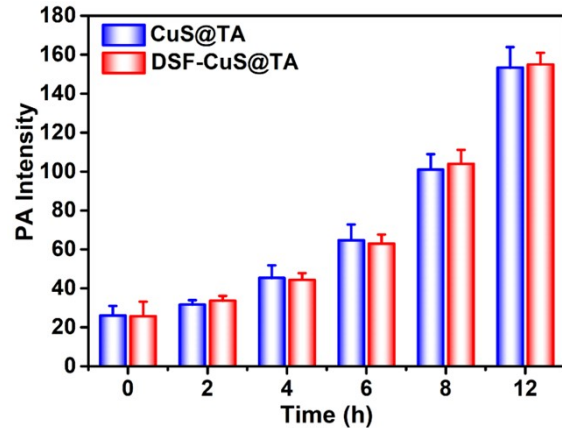


Fig. S22 The PA signal intensity of the tumor position.

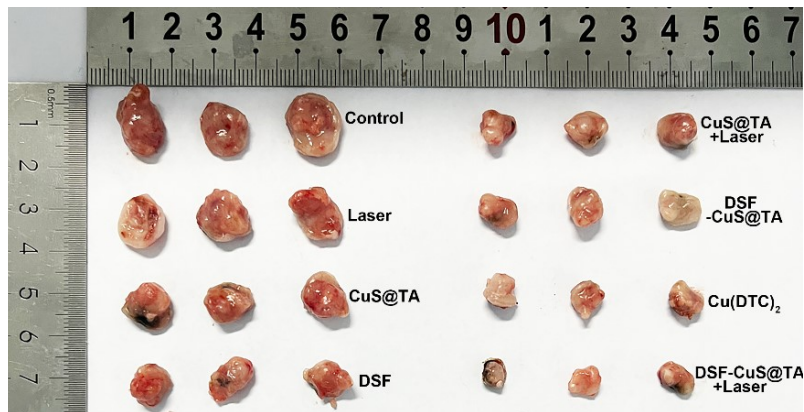


Fig. S23 Tumor photographs of 4T1 tumor-bearing mice in different treatment groups.

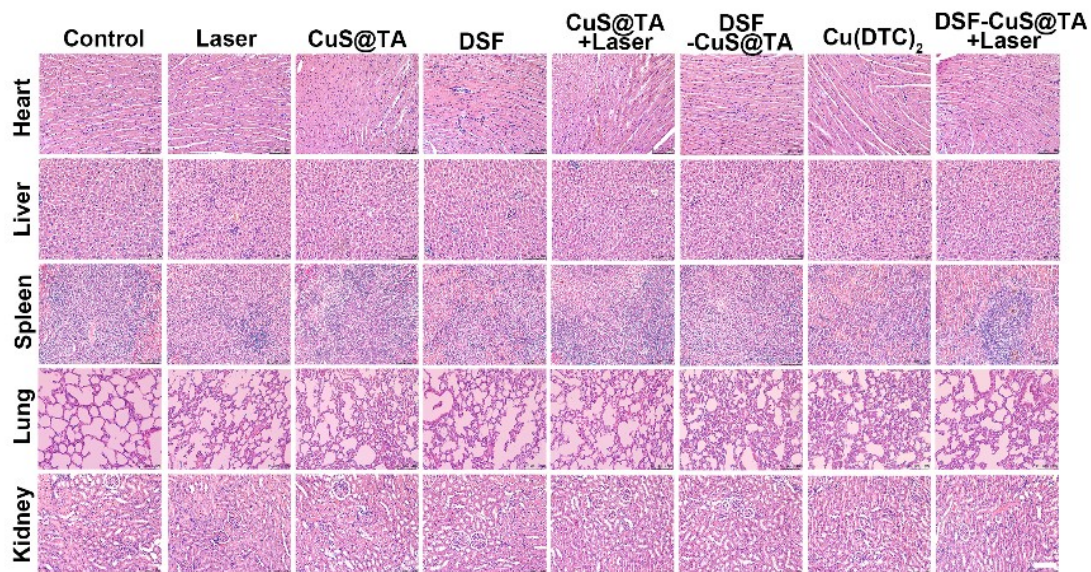


Fig. S24 H&E staining of major organs of 4T1 tumor-bearing mice in different groups. Scale bar, 100 μm .

Reference

1. H. Zhang, Q. Y. Zhang, Z. Y. Guo, K. Liang, C. Boyer, J. Liu, Z. H. Zheng, R. Amal, S. L. J. Yun and Z. Gu, *J Colloid. Interface Sci.*, 2022, **615**, 517–526.
2. M. Wen, J. Ouyang, C. Wei, H. Li, W. S. Chen and Y. N. Liu, *Angew. Chem. Int. Ed.*, 2019, **58**, 17425–17432.
3. H. S. Hsieh, R. Wu and C. T. Jafvert, *Environ. Sci. Technol.*, 2014, **48**, 11330–11336.